
Don’t Use Large Mini-Batches, Use Local SGD

Tao Lin

Sebastian U. Stich

Martin Jaggi

EPFL, Switzerland

Abstract

Mini-batch stochastic gradient methods are the current state of the art for large-scale distributed training of neural networks and other machine learning models. However, they fail to adapt to a changing communication vs computation trade-off in a system, such as when scaling to a large number of workers or devices. More so, the fixed requirement of communication bandwidth for gradient exchange severely limits the scalability to multi-node training e.g. in datacenters, and even more so for training on decentralized networks such as mobile devices. We argue that variants of local SGD, which perform several update steps on a local model before communicating to other nodes, offer significantly improved overall performance and communication efficiency, as well as adaptivity to the underlying system resources. Furthermore, we present a new hierarchical extension of local SGD, and demonstrate that it can efficiently adapt to several levels of computation costs in a heterogeneous distributed system.

1 Introduction

The workhorse training algorithm for most machine learning applications—including deep-learning—is stochastic gradient descent (SGD). This algorithm is highly preferred over its classic counterpart, i.e. full gradient descent (GD), not only because it offers much cheaper iterations, but also because it can be more efficient in total number of gradient evaluations. This efficiency gain of SGD over GD is very well studied and known to reach up to a factor of n for sum-structured problems, both in theory [1] and practice [2], for n being the training set size. When considering computational efficiency, there seems to be no reason to evaluate multiple stochastic gradients at the same time, such as done in mini-batch SGD. However, the latter algorithm can easily be parallelized among different workers, which makes it a better choice for modern distributed deep-learning applications for two reasons: (i) mini-batch SGD can exploit the compute parallelism locally available on modern computing devices such as GPUs. The second reason is that (ii) less frequent parameter updates do help alleviate the communication bottleneck between the worker devices, which is crucial in a distributed setting, in particular for large models.

Recent applications [3, 4] aim at reducing training time in the distributed setting by using many machines and by running SGD with dramatically larger mini-batch size than reported previously in the literature. However, we claim that in current training schemes this choice of large batches is often taken for the wrong reason, namely by not correctly trading-off the above two key points of local parallelism per device (e.g. GPU or mobile phone) on one hand, and communication efficiency between devices on the other hand. In particular, when scaling up the number of worker devices, the parallelism per device remains unchanged as a limiting factor, while the communication efficiency can decrease dramatically.

To solve this issue, and to allow adaptivity to the computation/communication trade-off, we propose to use novel variants of local SGD [5, 6, 7] on each worker. Local SGD scheme updates the parameters by averaging between the workers only after several local steps (without communication). We show

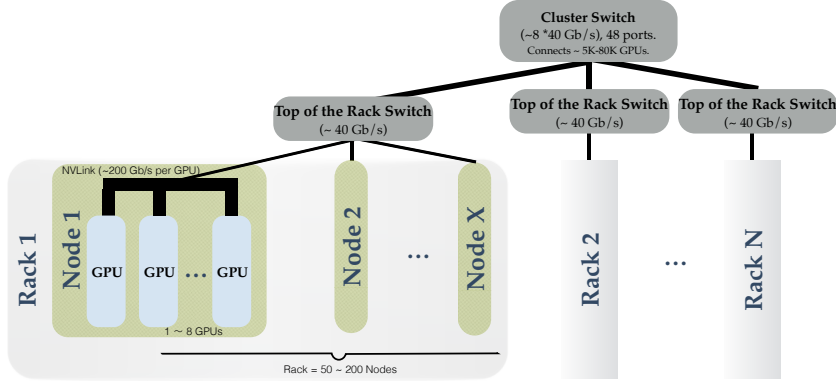


Figure 1: The hierarchical network architectures of a cluster in the data center. The GPUs within each node is connected via NVLink, while top of the rack switch and cluster switch provide much slow connection intra-/inter rack servers. The hierarchy can go up one or two levels further. After that, we have edge switches, that face the external network and are usually bulky (same bandwidth of cluster switches).

that tuning the number of steps between the communication rounds successfully decouples the two aspects of local parallelism and communication latency.

Furthermore, we leverage this idea to the more general setting of training on decentralized and heterogeneous systems, which is an increasingly important application area. Such systems have become common in industry, e.g. with GPUs or other accelerators grouped hierarchically within machines, racks or even at the level of several data-centers. A hierarchy network architecture in Figure 1 motivates the hierarchical extension of local SGD. Moreover, end-user devices such as mobile phones form huge heterogeneous networks, where the benefits of efficient distributed and data-local training of machine learning models, promises strong benefits in terms of data privacy.

Our main contributions are as follows:

- We propose a novel hierarchical extension of the local SGD training framework, further improving the adaptivity of local SGD to a wide range of real-world heterogeneous distributed systems. We show that in a realistic setting of training over multiple servers or datacenters, hierarchical local SGD offers significantly better performance compared to both local SGD and mini-batch SGD, in terms of communication efficiency to reach the same accuracy.
- We provide an extensive empirical performance study of local SGD training schemes for various state-of-the-art computer vision models, on distributed commodity hardware systems, and show clear empirical evidence of the advantage of this method compared to mini-batch SGD baselines. Our results show that local SGD significantly reduces the amount of communication while preserving the prediction accuracy. On ImageNet, local SGD outperforms the current large-batch training approach by a factor of at least $1.5 \times$ even in the non-hierarchical setting.

2 Related Work

While mini-batch and parallel SGD are very well studied [8, 9], there is still no clear theoretical understanding of local SGD variants. A parallel version of local SGD has been empirically studied in [7]. For a sub-class of convex models, [10] studies local SGD in the setting of a general graph of workers. The theoretical convergence advantage over mini-batch has remained elusive for a long time, see e.g. [11], until the very recent work of [12] which addresses the convergence rate in the convex case, and [13, 14] address the non-convex case. Here we focus on (synchronous) distributed SGD in large scale applications, under the plain map-reduce communication model. Our viewpoint is not specific to neural-network models, but applies to general sum structured distributed optimization objectives.

Asynchronous SGD algorithms [15, 16] aim to improve overall training time at the expense of additional noise introduced from asynchrony, i.e. updates coming from gradients computed at stale

weight vectors. [17] demonstrates that synchronous distributed SGD offers improved performance for deep learning workloads and is able to alleviate the staleness impact of asynchronous SGD. Current state-of-the-art distributed deep learning frameworks [18, 19, 20] resort to synchronized large-batch training, allowing scaling by adding more computational units and performing data-parallel synchronous SGD with mini-batches divided between devices. In order to improve the overall efficiency of mini-batch SGD training, those methods are restricted to increasing the batch size, while keeping the workload constant on each device. It has been shown that training with large batch size (e.g. batch size $> 10^3$ for the case of ImageNet) typically degrades the performance both in terms of training and test error [3, 21, 22, 23, 24, 25]. [3] suggests performing a “learning rate warm-up” phase with linear scaling of the step-size, successfully training ImageNet with a ResNet-50 network with batch size 8K (to the level of 76.26% accuracy).

For training in a massively distributed scenario, the work of [26, 27, 28] introduces the setting of federated learning. While other stochastic approaches such as e.g. [29, 30], require iid distributed data, this is not required in the federated setting. However, none of these algorithms address the task of training on a multi-level heterogeneous system. Another promising line of research addressing the communication bottleneck of large scale training is to use quantization [31, 32, 33] or more aggressive sparsification [34, 35, 36] of gradients. These techniques are orthogonal to our scheme and can offer promising savings when applied at the level of communication between the nodes.

3 Distributed Training

We consider standard sum-structured optimization problems of the form $\min_{\mathbf{w} \in \mathbb{R}^d} \frac{1}{n} \sum_{i=1}^n f_i(\mathbf{w})$, where \mathbf{w} are the parameters of the model (e.g. neural network), and f_i is the loss function of the i -th training data example.

The mini-batch update of SGD is given by

$$\mathbf{w}_{t+1} := \mathbf{w}_t - \gamma_t \left[\frac{1}{|\mathcal{I}_t|} \sum_{i \in \mathcal{I}_t} \nabla f_i(\mathbf{w}_t) \right], \quad (1)$$

where $\mathcal{I}_t \subseteq [n]$ is a subset of indices of the n training datapoints, typically selected uniformly at random, and γ_t denotes the step-size. $B := |\mathcal{I}_t|$ denotes the batch size, and the three update schemes of SGD, mini-batch SGD and GD respectively can be represented by $B = 1, B$ and N . In the distributed setup, data examples are partitioned across K devices (such as GPUs or cloud compute nodes), each only having access to its local training data. The workhorse algorithm in this setting is again mini-batch SGD,

$$\mathbf{w}_{t+1} := \mathbf{w}_t - \gamma_t \left[\frac{1}{K|\mathcal{I}_t^k|} \sum_{k=1}^K \sum_{i \in \mathcal{I}_t^k} \nabla f_i(\mathbf{w}_t) \right], \quad (2)$$

where now the mini-batch of the k -th device is formed from local data \mathcal{I}_t^k , and the K devices compute gradients in parallel and then synchronize the local gradients by averaging.

3.1 Local SGD

In contrast to mini-batch SGD, local SGD performs local sequential updates on each device, before aggregating the updates between the K devices, as illustrated in Figure 2.

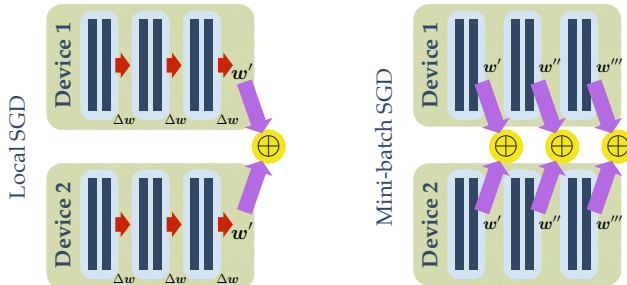


Figure 2: One round of local SGD (left) versus mini-batch SGD (right). In both settings $B_{\text{loc}} = 2$. For the local variant, we have $H = 3$ local steps. Local parameter updates are depicted in red, whereas global averaging (synchronization) is depicted in purple.

Each worker k iteratively samples small mini-batches of fixed size B_{loc} , from its local data \mathcal{I}^k . It then sequentially performs $H \geq 1$ local parameter updates, before performing global parameter aggregation with the other devices. Therefore, per synchronization/communication, local SGD accesses $B_{\text{glob}} = H \cdot B_{\text{loc}}$ training examples (gradient computations) on each device.

Formally, one round of local SGD can be described as

$$\mathbf{w}_{(t)+H}^k := \mathbf{w}_{(t)}^k - \sum_{h=1}^H \gamma_{(t)} \left[\frac{1}{B_{\text{loc}}} \sum_{i \in \mathcal{I}_{(t)+h-1}^k} \nabla f_i(\mathbf{w}_{(t)+h-1}^k) \right], \quad (3)$$

where $\mathbf{w}_{(t)+h}^k$ denotes the local model on machine k after t global synchronization rounds and subsequent h local steps. After H local updates the synchronized global model $\mathbf{w}_{(t+1)}^k$ is obtained by averaging $\mathbf{w}_{(t)+H}^k$ among the K workers as in an all-reduce communication pattern

$$\mathbf{w}_{(t+1)}^k := \mathbf{w}_{(t)}^k - \frac{1}{K} \sum_{k=1}^K (\mathbf{w}_{(t)}^k - \mathbf{w}_{(t)+H}^k). \quad (4)$$

Later, we will modify the update scheme of local SGD in (4) to include momentum, see Appendix E.1.1 for details.

3.2 Hierarchical Local SGD

Real world systems come with different communication bandwidths on several levels. In this scenario, we propose to employ local SGD on each level of the hierarchy, adapted to each corresponding computation vs communication trade-off. The resulting scheme, hierarchical local SGD, offers significant benefits in system adaptivity and performance as we will see in the rest of the paper.

As the guiding example, we consider compute clusters which typically allocate a large number of GPUs grouped over several machines, and refer to each group as a GPU-block. Hierarchical local SGD continuously updates the local models on each GPU for a number of H *local update steps* before a (fast) synchronization within a GPU-block. On the outer level, after H^b such *block update steps*, a (slower) global synchronization over all GPU-blocks is performed. The complete procedure is formalized as

$$\begin{aligned} \mathbf{w}_{[(t)+l]+H}^k &:= \mathbf{w}_{[(t)+l]}^k - \sum_{h=1}^H \gamma_{[(t)]} \left(\frac{1}{B_{\text{loc}}} \sum_{i \in \mathcal{I}_{[(t)+l]+h-1}^k} \nabla f_i(\mathbf{w}_{[(t)+l]+h-1}^k) \right) \\ \mathbf{w}_{[(t)+l+1]}^k &:= \mathbf{w}_{[(t)+l]}^k - \frac{1}{K_i} \sum_{k=1}^{K_i} (\mathbf{w}_{[(t)+l]}^k - \mathbf{w}_{[(t)+l]+H}^k) \\ \mathbf{w}_{[(t+1)]}^k &:= \mathbf{w}_{[(t)]}^k - \frac{1}{K} \sum_{k=1}^K (\mathbf{w}_{[(t)]}^k - \mathbf{w}_{[(t)+H^b]}^k) \end{aligned} \quad (5)$$

where $\mathbf{w}_{[(t)+l]+H}^k$ indicates the model after l block update steps and H local update steps, and K_i is the number of GPUs on the GPU-block i .

As the number of devices grows to the thousands [3, 4], the difference between ‘within’ and ‘between’ block communication efficiency becomes more drastic. Thus, the performance benefits of our adaptive scheme compared to flat & large mini-batch SGD will be even more pronounced.

3.3 Convergence Theory of Local SGD

The main advantage of local SGD over mini-batch SGD is the drastic reduction in the amount of communication, when accessing the same number of datapoints or gradients. However, this advantage would be in vain if the convergence of local SGD would be slower than the one of mini-batch SGD. In the following section, we, therefore, consider the theoretical convergence properties for local SGD.

First we discuss the convex setting. It is well-known that an individual local run of SGD converges as $\mathcal{O}((THB_{\text{loc}})^{-1})$, see e.g. [37]. By convexity, we can derive that averaging K instances of such

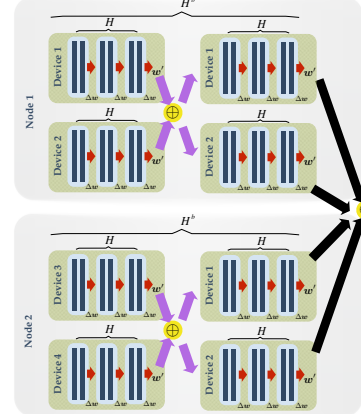


Figure 3: The illustration of hierarchical local SGD. We set $B_{\text{loc}} = 2$, and have $H = 3$ local steps and $H^b = 2$ block steps. Local parameter updates are depicted in red, whereas block and global synchronization is depicted in purple and black respectively.

local SGD executions will only improve the attained training objective value. However, this simple argument is not enough to quantify the speed-up of local SGD, i.e. does not allow to incorporate K in the rate. This is still an active area of research (cf. also [11, 12]). Stich [12] recently showed linear speed-up, i.e. convergence at rate $\mathcal{O}((KTHB_{\text{loc}})^{-1})$ for strongly convex and smooth objective functions.

Two recent theoretical contributions shed some light on local SGD in the non-convex setting. For smooth objective functions, Zhou et al. [13] show a rate $\mathcal{O}((KTB_{\text{loc}})^{-1/2})$ which only coincides in the extreme case $H = 1$ with the rate of mini-batch SGD. Building on the techniques from [12], Yu et al. [14] improve the rate to $\mathcal{O}((HKTB_{\text{loc}})^{-1/2})$.

All those results assume a fixed communication frequency H . However, it is not clear yet whether this is the best choice in general. Intuitively, one would expect when the diversity of the local sequences $\mathbf{w}_{(t)+h}^k$ is small, for instance measured as $\frac{1}{K} \sum_{k=1}^K \mathbb{E} \|\bar{\mathbf{w}}_{(t)+h}^k - \mathbf{w}_{(t)+h}^k\|^2$ for $\bar{\mathbf{w}}_{(t)+h}^k := \frac{1}{K} \sum_{k=1}^K \mathbf{w}_{(t)+h}^k$; then one has to communicate less frequently. On the other hand when the difference between the sequences is larger (such as expected at the beginning of the training process) then one should communicate updates more frequently. Zhang and coauthors [7] empirically studied the effect of the averaging frequency on the quality of the solution for some problem cases. They argue that more frequent averaging at the beginning of the optimization can help and bring forward a theoretical illustration that supports this finding. Also in [10] the authors argue to average more frequently at the beginning. Thus, we will adopt such a strategy later in the experiments.

4 Experimental Results

In this section, we empirically compare mini-batch SGD and the proposed (hierarchical) local SGD. First we describe the experimental setup.

Datasets. For the experiments we use the following popular image classification tasks.

- CIFAR-10/100 [38]. Each consist of a training set of 50K and a test set of 10K color images of 32×32 pixels, as well as 10 and 100 target classes respectively. We adopt the standard data augmentation scheme and preprocessing of [39, 40].
- ImageNet [41]. The ILSVRC 2012 classification dataset consists of 1.28 million images for training, and 50K for validation, with 1K target classes. We use ImageNet-1k [42] and adopt the same data preprocessing and augmentation scheme as in [39, 43, 44]. The network input image is a 224×224 pixel random crop from augmented images, with per-pixel mean subtracted.

Model Selection. We use ResNet-20 [39] on CIFAR-10/100 to investigate the performance of (hierarchical) local SGD, and then use ResNet-50 on the challenging ImageNet to investigate the accuracy and scalability of (hierarchical) local SGD. We also run experiments on Densenet [45] and WideResNet [46] to demonstrate the generalization ability of local SGD for different models.

Model Initialization. We here only mention some shared strategies for model initialization. Some model-specific initialization schemes, e.g., the use of momentum scheme, can be found in the experimental sections below. For all models, we use a weight decay λ of $1e-4$ and, following [39], we do not apply weight decay on the learnable Batch Normalization (BN) coefficients. For the weight initialization we follow [3] where we adopt the initialization introduced by [47] for convolution layers, and initialize fully-connected layer from a zero-mean Gaussian distribution with the standard deviation of 0.01. For the BN for distributed training we again follow [3] and compute the BN statistics independently for each worker.

Implementation and platform. We implement¹ (hierarchical) local SGD in PyTorch [19], with a flexible configuration of the machine topology supported by Kubernetes. The cluster consists of 15 $2 \times$ Intel Xeon E5-2680 v3 servers and has 30 NVIDIA TITAN Xp GPUs in total. In the rest of the paper, we use $a \times b$ -GPU to denote the topology of the cluster, i.e., a nodes and each with b GPUs.

¹ Our code will be made publicly available.

4.1 Training on CIFAR-10/100

In our first experiments with (hierarchical) local SGD we train ResNet-20 with $K = 2$ GPUs. We show that *local SGD is an easy plugin alternative for mini-batch SGD, with significantly improved communication efficiency and guaranteed performance*.

The experiment follow the common mini-batch SGD training scheme for CIFAR [39, 43] and all competing methods access the same total amount of data samples regardless of the ratio of local steps or block steps. More precisely, the training procedure is terminated when the distributed algorithms have accessed the same number of samples as a standalone worker would access in 300 epochs. The data is partitioned among the GPUs and reshuffled globally every epoch. The local mini-batches are then sampled among the local data available on each GPU. The training procedure is kept consistent across the (hierarchical) local SGD experiments, and unless stated otherwise no specific treatments, e.g., use a specific learning rate scheme, prolong the training epochs, are adopted to enhance the generalization performance.

4.1.1 Local SGD Training

For CIFAR-10, we run local SGD training on 2 servers, each having 1 GPU. We use ResNet-20 with a learning rate scheme as in [39], where the initial learning rate starts from 0.1 and is divided by 10 when the model has accessed 50% and 75% of the total number of training samples. In addition to this, the momentum parameter is set to 0.9 without dampening, and applied independently to each local model².

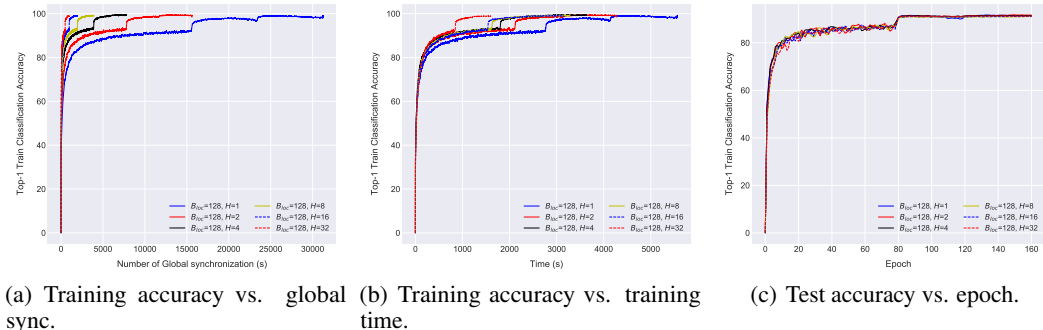


Figure 4: Training **CIFAR-10** with **ResNet-20** via **local SGD** (2×1 -GPU). The local batch size B_{loc} is fixed to 128, and the local step is varied from 1 to 32. All the experiments are under the same training configurations.

Better communication efficiency, with guaranteed test accuracy. Figure 4 shows that *local SGD is significantly more communication efficient while guaranteeing the same accuracy and enjoys faster convergence speed*. In Figure 4, the local models use a fixed local mini-batch size B_{loc} for all updates. All methods run for the same number of total gradient computations. Mini-batch SGD—the baseline method for comparison—is a special case of local SGD with $H = 1$, with full global model synchronization for each local update. We see that local SGD with $H > 1$, as illustrated in Figure 4(a), by design does H times less global model synchronizations, alleviating the communication bottleneck while accessing the same number of samples. The impact of local SGD training upon the total training time is more significant for larger local step H (i.e., Figure 4(b)), resulting in an at least $3 \times$ speed-up when comparing mini-batch $H = 1$ to local SGD with $H = 32$. The reached final training accuracy remains stable across different H values, and there is no difference or negligible difference with regard to test accuracy (Figure 4(c)). The analogue experiments for the CIFAR-100 datasets are provided in the supplementary material, as well as the performance of local SGD on DenseNet and WideResNet in Table 5.

Better generalization performance than “large batch training”. Table 1 demonstrates that *local SGD has a much better generalization performance than mini-batch SGD, when accessing the same number of samples (gradient computations) per device per global synchronization*. Large-batch

² The investigation of local momentum and global momentum can be found in the supplementary material.

training methods proposed different tricks to overcome convergence problems, including scaling the learning rate and gradual warmup [3]. Table 1 shows that mini-batch SGD with large-batch training could still be a severe issue; while local SGD naturally solves this problem by updating the local model with many local update steps, which is verified by the stable test performances of local SGD across different H . An investigation of extreme training cases of local SGD when $H \gg 1$ can be found in Table 6 and Table 7 in the supplementary material.

Table 1: Training **CIFAR-10** with **ResNet-20** via **local SGD** (2×1 -GPU). The test top-1 accuracy of mini-batch SGD and local SGD is reported, for a fixed number of accessed samples per synchronization B_{glob} . Note that local SGD will always fix the batch size $B_{\text{loc}} = 128$ but vary the number of local update steps H , while mini-batch SGD always keeps $H = 1$ and $B_{\text{loc}} = B_{\text{glob}}$. The reported results are the average of three runs. Variants with * indicate the use of large-batch learning tricks [3] (c.f. supplementary material), which we also compare to the corresponding default configurations for completeness and fair comparison.

	$B_{\text{glob}} = 128$	$B_{\text{glob}} = 256$	$B_{\text{glob}} = 512$	$B_{\text{glob}} = 1024$	$B_{\text{glob}} = 2048$	$B_{\text{glob}} = 4096$
local SGD*	92.47 \pm 0.16	92.31 \pm 0.06	92.27 \pm 0.04	92.05 \pm 0.17	91.63 \pm 0.13	91.57 \pm 0.19
mini-batch SGD*	92.47 \pm 0.16	92.25 \pm 0.18	92.03 \pm 0.40	92.02 \pm 0.11	86.57 \pm 7.57	15.95 \pm 3.05
local SGD	92.04 \pm 0.50	92.00 \pm 0.13	91.86 \pm 0.15	92.03 \pm 0.39	91.85 \pm 0.16	91.67 \pm 0.02
mini-batch SGD	92.04 \pm 0.50	91.94 \pm 0.25	91.79 \pm 0.32	90.11 \pm 0.57	89.48 \pm 0.73	57.58 \pm 38.10

4.1.2 Hierarchical Local SGD Training

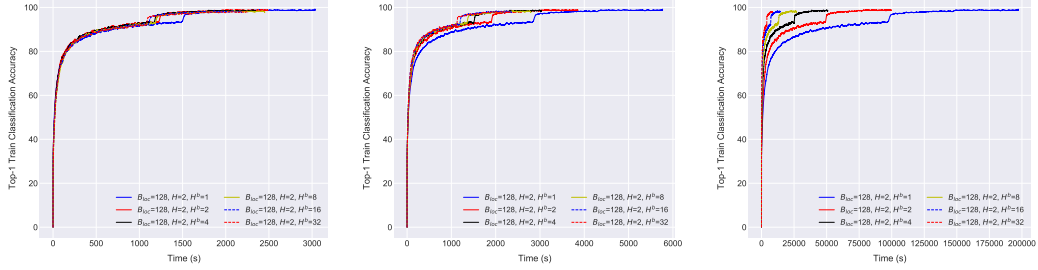
Now we move to our proposed training scheme for distributed heterogeneous systems. In our experimental setup we try to mimic the real world setting where several compute devices such as GPUs are grouped over different servers, and where network bandwidth (e.g. Ethernet) limits the communication of updates of large models.

Table 2: Training **CIFAR-10** with **ResNet-20** via **local SGD** on a 5×2 -GPU cluster. The local batch size B_{loc} is fixed to 128 with $H^b = 1$, and we scale the local step H from 1 to 1024. The reported results are the average of three runs and all the experiments are under the same training configurations without specific tuning.

H	1	2	4	8	16	32	64	128	256	512	1024
Training Time (minutes)	20.07	13.95	10.48	9.20	8.57	8.32	9.22	9.23	9.50	10.30	10.65

Training time vs. local number of steps. Table 2 examines the performance of local SGD in terms of training time. The communication traffic comes from the global synchronization over 5 nodes, each having 2 GPUs. We can witness that the large number of local update steps over the “datacenter” scenario would even reduce the communication benefits brought by local updates. This slight performance degradation might result from the increased synchronization time needed by independent local processes (e.g., they have asynchronous local update status and distributed local processes even need longer time to synchronize again, so as increasing the communication cost from the other aspect.). *Hierarchical local SGD with inner node synchronization reduces the difficulty of synchronizing over complex heterogeneous environment, and hence enhances the overall system performance of the synchronization. The benefits are further pronounced when scaling up the cluster size.*

Hierarchical local SGD shows high tolerance to network delays. Even in our small-scale experiment of two servers and each with two GPUs, *hierarchical local SGD still shows its ability of significantly reduce the communication cost by increasing the number of block step H^b (for a fixed H), with trivial performance degradation. Moreover, hierarchical local SGD with sufficient number of block steps offers strong robustness to network delays.* For example, for fixed $H = 2$, by increasing the number of H^b , i.e., reducing the number of global synchronizations over all models, we obtain a significant gain in training time as in Figure 5(a). The impact of a network of slower communication is further studied in Figure 5(b), where the training is simulated in a realistic scenario and each global communication round comes with an additional delay of 1 second. Surprisingly, even for the global synchronization with straggling workers and has occurred a much more severe 50 seconds delay per global communication round, Figure 5(c) demonstrate that a large number of block steps (e.g. $H^b = 16$) still manages to fully overcome the communication bottleneck with no/trivial performance damage.



(a) Training accuracy vs. time. (b) Training accuracy vs. time. (c) Training accuracy vs. time. $H = 2$ local steps. $H = 2$ local steps with 1 second $H = 2$ local steps with 50 seconds delay for each global synchronization. $H = 2$ local steps with 50 seconds delay for each global synchronization.

Figure 5: The performance of **hierarchical local SGD** trained on **CIFAR-10** with **ResNet-20** (2×2 -GPU). Each GPU block of the hierarchical local SGD has 2 GPUs, and we have 2 blocks in total. Each figure fixes the number of local steps but varies the number of block steps from 1 to 32. All the experiments are under the same training configurations without specific tuning.

Table 3: The performance of training **CIFAR-10** with **ResNet-20** via **hierarchical local SGD** on a 10-GPU Kubernetes cluster. Each GPU block of the hierarchical local SGD has 2 GPUs, and we have 5 blocks in total. The configuration of hierarchical local SGD satisfies $HH^b = 16$. These SGD variants either synchronize within each node or over all GPUs, and the communication cost is estimated by only considering $HH^b = 16$ model updates during the training (the update could come from a different level of the synchronizations). The reported results are the average of three runs and all the experiments are under the same training configurations without specific tuning.

	$H = 1, H^b = 16$	$H = 2, H^b = 8$	$H = 4, H^b = 4$	$H = 8, H^b = 2$	$H = 16, H^b = 1$
# of sync. over nodes	1	1	1	1	1
# of sync. within node	15	7	3	1	0
Test top-1 accuracy (%)	90.37 ± 0.16	89.94 ± 0.13	89.23 ± 0.24	89.10 ± 0.03	88.45 ± 0.22
Training time (minutes)	19.62	17.08	15.98	15.55	15.05

Hierarchical local SGD naturally supports to scale larger and perform better. Table 3 compares the mini-batch SGD with hierarchical local SGD for fixed $HH^b = 16$. We can observe that hierarchical local SGD with sufficient number of block steps can alleviate the accuracy degradation. More precisely, when HH^b is fixed, hierarchical local SGD with more frequent inner-node synchronizations ($H^b > 1$) outperforms local SGD ($H^b = 1$), while still maintaining the benefits of significantly reduced communication by the inner synchronizations within each node. In summary, as witnessed by Tables 2 and 3, *hierarchical local SGD outperforms both local SGD and mini-batch SGD in terms of training speed as well as model performance*, especially for the training across nodes where inter-node connection is slow but intra-node communication is more efficient.

4.2 Training on ImageNet-1k

While in Section 4.1 above we have explored the performance of (hierarchical) local SGD on the CIFAR-10 dataset, this section demonstrates that local SGD is a competitive alternative to the current large-batch ImageNet training methods. Figure 6(a) and Figure 6(b) below show that we can efficiently (at least $1.5 \times$) train state-of-the-art ResNet-50 [39, 3, 48] for ImageNet via local SGD on a 15×2 -GPU Kubernetes cluster.

We limit ResNet-50 training to 90 passes over the data in total, and the data is disjointly partitioned and is re-shuffled globally every epoch. We adopt the large batch learning tricks [3], and linearly scale the learning rate based on # of GPUs $\times \frac{0.1}{256}$ where 0.1 and 256 is the base learning rate and mini-batch size respectively for standard single GPU training. The local mini-batch size is set to 128. For learning rate scaling, we perform gradual warmup for the first 5 epochs, and decay the scaled learning rate by the factor of 10 when local models have access 30, 60, 80 epochs of training samples respectively. Moreover, in our ImageNet experiment, the initial phase of local SGD training follows

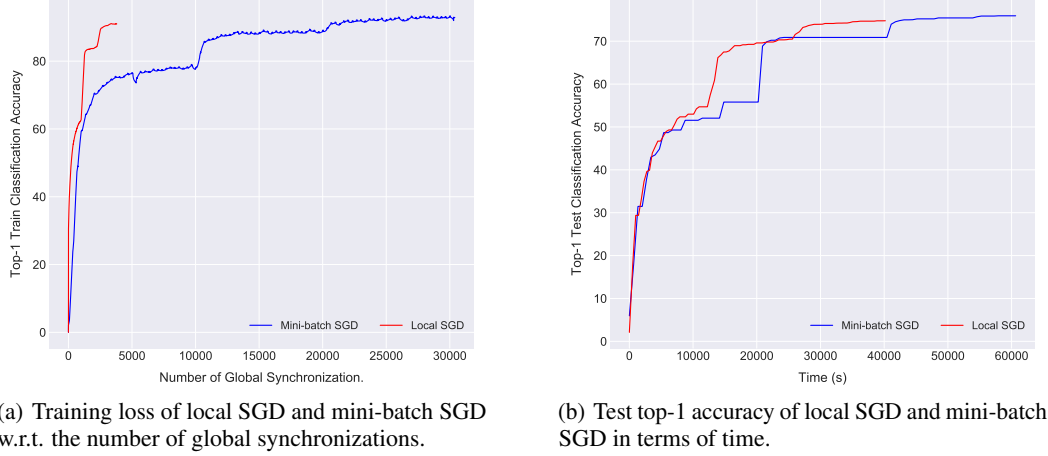


Figure 6: The performance of **local SGD** trained on **ImageNet-1k** with **ResNet-50** on a 15×2 -GPU cluster. We evaluate the model performance on test dataset after each complete accessing of the whole training samples. We apply the large batch learning tricks [3] to the ImageNet for these two methods. For local SGD, the local step is set to $H = 8$.

the theoretical assumption mentioned in Subsection 3.3, and thus we gradually warmup the number of local steps from 1 to the expected local step H during the first few epochs of the training³.

5 Discussion

All of our experimental settings mentioned above are under a mild data assumption, i.e., the dataset will be globally shuffled per epoch and only a disjoint part of it will be accessed by the local model. It would be very interesting to check the scenario where each local model can only access to disjointly and (very) limited local data during the whole training process.

Moreover, the local SGD with large batch training tricks [3] and fixed local update step presents consistent state-of-the-art performance over the experiments. It is worthwhile to explore the even more effective learning rate schedules for (hierarchical) local SGD.

As local SGD could present better generalization than the current mini-batch SGD approach, it is promising to see if an adaptive local update step, could remove the necessity of using complex learning rate schedules. The adaptive local step here could refer to adjust the number of local update steps per global synchronization based on the current learning status. Furthermore, some work like [49, 50] leverage cyclic learning rate schedules either improving the anytime performance of deep neural network training, or ensembling multiple neural networks at no additional training cost. Adaptive local step for local SGD could be the other way to achieve these goals with significantly reduced training cost.

6 Conclusion

In this work, we leverage the idea of local SGD to the general setting of training on decentralized and heterogeneous environments. For this, we propose a hierarchical version of local SGD that can efficiently adapt to a wide range of real-world heterogenous systems. Furthermore, we empirically study local SGD on various state-of-the-art computer vision models, demonstrating the significantly improved overall performance and communication efficiency, both in the hierarchical as well as flat distributed training setting.

³ In our local SGD experiment for ImageNet, we found that exponentially increasing the local step from 1 by the factor of 2 (until reaching the expected local step number) performs well.

References

- [1] Shai Shalev-Shwartz, Yoram Singer, Nathan Srebro, and Andrew Cotter. Pegasos: Primal Estimated Sub-Gradient Solver for SVM. *Mathematical Programming*, 127(1):3–30, 2010.
- [2] Léon Bottou. Large-Scale Machine Learning with Stochastic Gradient Descent. In Yves Lechevallier and Gilbert Saporta, editors, *COMPSTAT'2010 - Proceedings of the 19th International Conference on Computational Statistics*, pages 177–187, 2010.
- [3] Priya Goyal, Piotr Dollár, Ross Girshick, Pieter Noordhuis, Lukasz Wesolowski, Aapo Kyrola, Andrew Tulloch, Yangqing Jia, and Kaiming He. Accurate, large minibatch sgd: Training imagenet in 1 hour. *arXiv preprint arXiv:1706.02677*, 2017.
- [4] Yang You, Zhao Zhang, James Demmel, Kurt Keutzer, and Cho-Jui Hsieh. Imagenet training in 24 minutes. *arXiv preprint arXiv:1709.05011*, 2017.
- [5] Ryan McDonald, Mehryar Mohri, Nathan Silberman, Dan Walker, and Gideon S. Mann. Efficient large-scale distributed training of conditional maximum entropy models. In Y. Bengio, D. Schuurmans, J. D. Lafferty, C. K. I. Williams, and A. Culotta, editors, *Advances in Neural Information Processing Systems 22*, pages 1231–1239. Curran Associates, Inc., 2009. URL <http://papers.nips.cc/paper/3881-efficient-large-scale-distributed-training-of-conditional-maximum-entropy-models.pdf>.
- [6] Martin Zinkevich, Markus Weimer, Lihong Li, and Alex J Smola. Parallelized stochastic gradient descent. In *Advances in neural information processing systems*, pages 2595–2603, 2010.
- [7] Jian Zhang, Christopher De Sa, Ioannis Mitliagkas, and Christopher Ré. Parallel SGD: When does averaging help? *arXiv*, 2016.
- [8] Martin Takáč, Avleen Bijral, Peter Richtárik, and Nathan Srebro. Mini-Batch Primal and Dual Methods for SVMs. In *ICML 2013 - Proceedings of the 30th International Conference on Machine Learning*, March 2013.
- [9] Martin A Zinkevich, Markus Weimer, Alex J Smola, and Lihong Li. Parallelized Stochastic Gradient Descent. *NIPS 2010: Advances in Neural Information Processing Systems 23*, pages 1–37, 2010.
- [10] Avleen S Bijral, Anand D Sarwate, and Nathan Srebro. On Data Dependence in Distributed Stochastic Optimization. *arXiv.org*, 2016.
- [11] Dan Alistarh, Christopher De Sa, and Nikola Konstantinov. The Convergence of Stochastic Gradient Descent in Asynchronous Shared Memory. *arXiv*, March 2018.
- [12] Sebastian U Stich. Local SGD converges fast and communicates little. *arXiv preprint arXiv:1805.09767*, 2018.
- [13] Fan Zhou and Guojing Cong. On the convergence properties of a k-step averaging stochastic gradient descent algorithm for nonconvex optimization. In *Proceedings of the Twenty-Seventh International Joint Conference on Artificial Intelligence, IJCAI-18*, pages 3219–3227. International Joint Conferences on Artificial Intelligence Organization, 7 2018. doi: 10.24963/ijcai.2018/447. URL <https://doi.org/10.24963/ijcai.2018/447>.
- [14] Hao Yu, Sen Yang, and Shenghuo Zhu. Parallel restarted SGD for non-convex optimization with faster convergence and less communication. *arXiv preprint arXiv:1807.06629*, 2018.
- [15] Trishul M Chilimbi, Yutaka Suzue, Johnson Apacible, and Karthik Kalyanaraman. Project adam: Building an efficient and scalable deep learning training system. In *OSDI*, volume 14, pages 571–582, 2014.
- [16] Jeffrey Dean, Greg Corrado, Rajat Monga, Kai Chen, Matthieu Devin, Mark Mao, Andrew Senior, Paul Tucker, Ke Yang, Quoc V Le, et al. Large scale distributed deep networks. In *Advances in neural information processing systems*, pages 1223–1231, 2012.

- [17] Jianmin Chen, Xinghao Pan, Rajat Monga, Samy Bengio, and Rafal Jozefowicz. Revisiting distributed synchronous sgd. *arXiv preprint arXiv:1604.00981*, 2016.
- [18] Martín Abadi, Ashish Agarwal, Paul Barham, Eugene Brevdo, Zhifeng Chen, Craig Citro, Greg S Corrado, Andy Davis, Jeffrey Dean, Matthieu Devin, et al. Tensorflow: Large-scale machine learning on heterogeneous distributed systems. *arXiv preprint arXiv:1603.04467*, 2016.
- [19] Adam Paszke, Sam Gross, Soumith Chintala, Gregory Chanan, Edward Yang, Zachary DeVito, Zeming Lin, Alban Desmaison, Luca Antiga, and Adam Lerer. Automatic differentiation in PyTorch. 2017.
- [20] Frank Seide and Amit Agarwal. CNTK: Microsoft’s open-source deep-learning toolkit. In *Proceedings of the 22nd ACM SIGKDD International Conference on Knowledge Discovery and Data Mining*, pages 2135–2135. ACM, 2016.
- [21] Kai Chen and Qiang Huo. Scalable training of deep learning machines by incremental block training with intra-block parallel optimization and blockwise model-update filtering. In *Acoustics, Speech and Signal Processing (ICASSP), 2016 IEEE International Conference on*, pages 5880–5884. IEEE, 2016.
- [22] Elad Hoffer, Itay Hubara, and Daniel Soudry. Train longer, generalize better: closing the generalization gap in large batch training of neural networks. *arXiv preprint arXiv:1705.08741*, 2017.
- [23] Nitish Shirish Keskar, Dheevatsa Mudigere, Jorge Nocedal, Mikhail Smelyanskiy, and Ping Tak Peter Tang. On large-batch training for deep learning: Generalization gap and sharp minima. *arXiv preprint arXiv:1609.04836*, 2016.
- [24] Mu Li. *Scaling distributed machine learning with system and algorithm co-design*. PhD thesis, Intel, 2017.
- [25] Mu Li, Tong Zhang, Yuqiang Chen, and Alexander J Smola. Efficient mini-batch training for stochastic optimization. In *Proceedings of the 20th ACM SIGKDD international conference on Knowledge discovery and data mining*, pages 661–670. ACM, 2014.
- [26] Jakub Konecný, Brendan McMahan, and Daniel Ramage. Federated optimization: Distributed optimization beyond the datacenter. *arXiv preprint arXiv:1511.03575*, 2015.
- [27] Jakub Konecný, H Brendan McMahan, Felix X Yu, Peter Richtarik, Ananda Theertha Suresh, and Dave Bacon. Federated learning: Strategies for improving communication efficiency. *arXiv preprint arXiv:1610.05492*, 2016.
- [28] Brendan McMahan, Eider Moore, Daniel Ramage, Seth Hampson, and Blaise Aguera y Arcas. Communication-efficient learning of deep networks from decentralized data. In *Artificial Intelligence and Statistics*, pages 1273–1282, 2017.
- [29] Sixin Zhang, Anna E Choromanska, and Yann LeCun. Deep learning with Elastic Averaging SGD. In *NIPS 2015 - Advances in Neural Information Processing Systems 28*, pages 685–693, 2015.
- [30] Jialei Wang, Weiran Wang, and Nathan Srebro. Memory and Communication Efficient Distributed Stochastic Optimization with Minibatch Prox. In *ICML 2017 - Proceedings of the 34th International Conference on Machine Learning*, pages 1882–1919. June 2017.
- [31] Dan Alistarh, Demjan Grubic, Jerry Li, Ryota Tomioka, and Milan Vojnovic. QSGD: Communication-efficient SGD via gradient quantization and encoding. In I. Guyon, U. V. Luxburg, S. Bengio, H. Wallach, R. Fergus, S. Vishwanathan, and R. Garnett, editors, *NIPS - Advances in Neural Information Processing Systems 30*, pages 1709–1720. Curran Associates, Inc., 2017. URL <http://papers.nips.cc/paper/6768-qsgd-communication-efficient-sgd-via-gradient-quantization-and-encoding.pdf>.

[32] Shuchang Zhou, Yuxin Wu, Zekun Ni, Xinyu Zhou, He Wen, and Yuheng Zou. Dorefa-net: Training low bitwidth convolutional neural networks with low bitwidth gradients. *arXiv preprint arXiv:1606.06160*, 2016.

[33] Wei Wen, Cong Xu, Feng Yan, Chunpeng Wu, Yandan Wang, Yiran Chen, and Hai Li. Terngrad: Ternary gradients to reduce communication in distributed deep learning. *arXiv preprint arXiv:1705.07878*, 2017.

[34] Alham Fikri Aji and Kenneth Heafield. Sparse communication for distributed gradient descent. *arXiv preprint arXiv:1704.05021*, 2017.

[35] Yujun Lin, Song Han, Huizi Mao, Yu Wang, and William J Dally. Deep gradient compression: Reducing the communication bandwidth for distributed training. *arXiv preprint arXiv:1712.01887*, 2017.

[36] Nikko Strom. Scalable distributed dnn training using commodity gpu cloud computing. In *INTERSPEECH*, pages 1488–1492. ISCA, 2015. URL <http://dblp.uni-trier.de/db/conf/interspeech/interspeech2015.html#Strom15>.

[37] Simon Lacoste-Julien, Mark Schmidt, and Francis Bach. A simpler approach to obtaining an $o(1/t)$ convergence rate for the projected stochastic subgradient method. *arXiv preprint arXiv:1212.2002*, 2012.

[38] Alex Krizhevsky and Geoffrey Hinton. Learning multiple layers of features from tiny images. 2009.

[39] Kaiming He, Xiangyu Zhang, Shaoqing Ren, and Jian Sun. Deep residual learning for image recognition. In *Proceedings of the IEEE Conference on Computer Vision and Pattern Recognition*, pages 770–778, 2016.

[40] Gao Huang, Yu Sun, Zhuang Liu, Daniel Sedra, and Kilian Q Weinberger. Deep networks with stochastic depth. In *European Conference on Computer Vision*, pages 646–661. Springer, 2016.

[41] Olga Russakovsky, Jia Deng, Hao Su, Jonathan Krause, Sanjeev Satheesh, Sean Ma, Zhiheng Huang, Andrej Karpathy, Aditya Khosla, Michael Bernstein, et al. Imagenet large scale visual recognition challenge. *International Journal of Computer Vision*, 115(3):211–252, 2015.

[42] J. Deng, W. Dong, R. Socher, L.-J. Li, K. Li, and L. Fei-Fei. ImageNet: A Large-Scale Hierarchical Image Database. In *CVPR09*, 2009.

[43] Kaiming He, Xiangyu Zhang, Shaoqing Ren, and Jian Sun. Identity mappings in deep residual networks. In *European Conference on Computer Vision*, pages 630–645. Springer, 2016.

[44] Karen Simonyan and Andrew Zisserman. Very deep convolutional networks for large-scale image recognition. *arXiv preprint arXiv:1409.1556*, 2014.

[45] Gao Huang, Zhuang Liu, Kilian Q Weinberger, and Laurens van der Maaten. Densely connected convolutional networks. *arXiv preprint arXiv:1608.06993*, 2016.

[46] Sergey Zagoruyko and Nikos Komodakis. Wide residual networks. *arXiv preprint arXiv:1605.07146*, 2016.

[47] Kaiming He, Xiangyu Zhang, Shaoqing Ren, and Jian Sun. Delving deep into rectifiers: Surpassing human-level performance on imagenet classification. In *Proceedings of the IEEE international conference on computer vision*, pages 1026–1034, 2015.

[48] Yang You, Zhao Zhang, Cho-Jui Hsieh, and James Demmel. 100-epoch imagenet training with alexnet in 24 minutes. *arXiv preprint arXiv:1709.05011*, 2017.

[49] Ilya Loshchilov and Frank Hutter. Sgdr: stochastic gradient descent with restarts. *arXiv preprint arXiv:1608.03983*, 2016.

[50] Gao Huang, Yixuan Li, Geoff Pleiss, Zhuang Liu, John E Hopcroft, and Kilian Q Weinberger. Snapshot ensembles: Train 1, get m for free. *arXiv preprint arXiv:1704.00109*, 2017.

- [51] William Gropp, Ewing Lusk, and Anthony Skjellum. *Using MPI: portable parallel programming with the message-passing interface*, volume 1. MIT press, 1999.
- [52] Rajeev Thakur, Rolf Rabenseifner, and William Gropp. Optimization of collective communication operations in mpich. *The International Journal of High Performance Computing Applications*, 19(1):49–66, 2005.
- [53] Rolf Rabenseifner. Optimization of collective reduction operations. In *International Conference on Computational Science*, pages 1–9. Springer, 2004.

A The Algorithm of Local SGD and Hierarchical Local SGD

Algorithm 1 Local SGD

input: the initial model $\mathbf{w}_{(0)}$;
input: training data with labels \mathcal{I} ;
input: minibatch of size B_{loc} per local model;
input: step size η , and momentum m (optional);
input: number of synchronization steps T ;
input: number of local update steps H ;
input: number of nodes K .

1: synchronize and to have the same initial models $\mathbf{w}_{(0)}^k := \mathbf{w}_{(0)}$.
2: **for all** $k := 1, \dots, K$ **do in parallel**
3: **for** $t := 1, \dots, T$ **do**
4: **for** $h := 1, \dots, H$ **do**
5: sample a mini-batch from $\mathcal{I}_{(t)+h-1}^k$.
6: compute the gradient $\mathbf{g}_{(t)+h-1}^k := \frac{1}{B_{\text{loc}}} \sum_{i \in \mathcal{I}_{(t)+h-1}^k} \nabla f_i(\mathbf{w}_{(t)+h-1}^k)$.
7: update the local model to $\mathbf{w}_{(t)+h}^k := \mathbf{w}_{(t)+h-1}^k - \gamma_{(t)} \mathbf{g}_{(t)+h-1}^k$.
8: **end for**
9: all-reduce aggregation of the gradients $\Delta_{(t)}^k := \mathbf{w}_{(t)}^k - \mathbf{w}_{(t)+H}^k$.
10: with communication of the new global model $\mathbf{w}_{(t+1)}^k$ to all K nodes (synchronized):

$$\mathbf{w}_{(t+1)}^k := \mathbf{w}_{(t)}^k - \gamma_{(t)} \frac{1}{K} \sum_{i=1}^K \Delta_{(t)}^k$$

11: **end for**
12: **end for**

Algorithm 2 *Hierarchical Local SGD*

input: the initial model $\mathbf{w}_{[(0)]}$;
input: training data with labels \mathcal{I} ;
input: minibatch of size B_{loc} per local model;
input: step size η , and momentum m (optional);
input: number of synchronization steps T over nodes;
input: number of local update steps H ;
input: number of block update steps H^b ;
input: number of nodes K ;
input: number of nodes K' per GPU-block.
1: synchronize and to have the same initial models $\mathbf{w}_{[(0)]} := \mathbf{w}_{[(0)]}$.
2: **for all** $k := 1, \dots, K$ **do in parallel**
3: **for** $t := 1, \dots, T$ **do**
4: **for** $l := 1, \dots, H^b$ **do**
5: **for** $h := 1, \dots, H$ **do**
6: sample a mini-batch from $\mathcal{I}_{[(t)+l]+h-1}^k$.
7: compute the gradient $\mathbf{g}_{[(t)+l]+h-1}^k := \frac{1}{B_{\text{loc}}} \sum_{i \in \mathcal{I}_{[(t)+l]+h-1}^k} \nabla f_i(\mathbf{w}_{[(t)+l]+h-1}^k)$.
8: update the local model to $\mathbf{w}_{[(t)+l]+h}^k := \mathbf{w}_{[(t)+l]+h-1}^k - \gamma_{[(t)]} \mathbf{g}_{[(t)+l]+h-1}^k$.
9: **end for**
10: all-reduce aggregation of the gradients $\Delta_{[(t)+l]}^k := \mathbf{w}_{[(t)+l]}^k - \mathbf{w}_{[(t)+l]+H}^k$.
11: with communication of the new block model $\mathbf{w}_{[(t)+l+1]}^k$ to the K' block nodes:

$$\mathbf{w}_{[(t)+l+1]}^k := \mathbf{w}_{[(t)+l]}^k - \gamma_{[(t)]} \frac{1}{K'} \sum_{k=1}^{K'} \Delta_{[(t)+l]}^k,$$

where each GPU-level block will have a synchronized model.

12: **end for**
13: all-reduce aggregation of the gradients $\Delta_{[(t)]}^k := \mathbf{w}_{[(t)]}^k - \mathbf{w}_{[(t)+H^b]}^k$.
14: with communication of the new global model $\mathbf{w}_{[(t+1)]}^k$ to all K nodes:

$$\mathbf{w}_{[(t+1)]}^k := \mathbf{w}_{[(t)]}^k - \gamma_{[(t)]} \frac{1}{K} \sum_{i=1}^K \Delta_{[(t)]}^k$$

15: **end for**
16: **end for**

B Communication Schemes

This section evaluates the communication cost in terms of local update step and block update step, and formalizes the whole communication problem below.

Assume K computing devices uniformly distributed over K' servers, where each server has $\frac{K}{K'}$ devices. The hierarchical local SGD training procedure will access N total samples with local mini-batch size B , with H local update steps and H^b block update steps.

The MPI communication scheme [51] is introduced for communication cost evaluation. More precisely, we use general all-reduce, e.g., *recursive halving and doubling algorithm* [52, 53], for gradient aggregation among K computation device. For each all-reduce communication, it introduces $C \cdot \log_2 K$ communication cost, where C is the message transmission time plus network latency.

The communication cost under our hierarchical local SGD setting is mainly determined by local step and block step. The $\frac{K}{T}$ models within each server synchronize the gradients for every H local mini-batch, and it only performs global gradients aggregation of K local models after H^b block updates. Thus, the total number of synchronizations among compute devices is reduced to $\lceil \frac{N}{KB \cdot HH^b} \rceil$, and we can formulate the overall communication cost \tilde{C} as:

$$\tilde{C} \approx \left(\lceil \frac{N}{KB \cdot H} \rceil - \lceil \frac{N}{KB \cdot HH^b} \rceil \right) \cdot C_1 \cdot K' \log_2 \frac{K}{K'} + \lceil \frac{N}{KB \cdot HH^b} \rceil \cdot C_2 \log_2 K \quad (6)$$

where C_1 is the single message passing cost for compute devices within the same server, C_2 is the cost of that across servers, and obviously $C_1 \ll C_2$. We can easily witness that the number of block step H^b is more deterministic in terms of communication reduction than local step H . Empirical evaluations can be found in Section 4.1.2.

Also, note that our hierarchical local SGD is orthogonal to the implementation of gradient aggregation [3] optimized for the hardware, but focusing on overcoming the aggregation cost of a more general distributed scenarios, and can be easily integrated with any optimized all-reduce implementation.

C Large Batch Training Tricks

The work of [3] proposes common configurations to tackle large-batch training for the ImageNet dataset. We specifically refer to their crucial techniques w.r.t. learning rate as ‘‘large batch learning tricks’’ in our main text. For a precise definition, this is formalized by the following two configurations:

- **Scaling the learning rate:** When the mini-batch size is multiplied by k , multiply the learning rate by k .
- **Learning rate gradual warmup:** We gradually ramp up the learning rate from a small to a large value. In (our) experiments, with a large mini-batch of size kn , we start from a learning rate of η and increment it by a constant amount at each iteration such that it reaches $\hat{\eta} = k\eta$ after 5 epochs. More precisely, the incremental step size for each iteration is calculated from $\frac{\hat{\eta} - \eta}{5N/(K)}$, where N is the number of total training samples, K is the number of computing units and B_{loc} is the local mini-batch size.

D Additional Experimental Results

D.1 Model Selection

Table 4: Scaling ratio for different models.

Model	Communication # parameters	Computation # flops per image	Computation/Communication scaling ratio
ResNet-20 (CIFAR-10)	0.27 million	0.041 billion	151.85
ResNet-20 (CIFAR-100)	0.27 million	0.041 billion	151.85
ResNet-50 (ImageNet-1k)	25.00 million	7.7 billion	308.00
DenseNet-40-12 (CIFAR-10)	1.06 million	0.28 billion	264.15
DenseNet-40-12 (CIFAR-100)	1.10 million	0.28 billion	254.55
WideResNet-28-10 (CIFAR-10)	36.48 million	5.24 billion	143.64
WideResNet-28-10 (CIFAR-100)	36.54 million	5.24 billion	143.40

The scaling ratio [4] identifies the ratio between computation and communication, wherein DNN models, the computation is proportional to the number of floating point operations required for processing an input while the communication is proportional to model size (or the number of parameters).

Our local SGD training scheme will show more advantages over models with small “computation and communication scaling ratio”.

D.2 Local SGD Training Results

D.2.1 An Evaluation of Mini-batch SGD and Local SGD on Different Models

Table 5 demonstrates an example that we can easily train state-of-the-art compute vision models through local SGD, with significantly reduced training time.

Table 5: A complete performance demonstration of two training schemes (i.e., **mini-batch SGD** and **local SGD**) on different models for **CIFAR-10** and **CIFAR-100** (2×1 -GPU). Note that regardless of the training scheme, the model is trained from the same hyper-parameter configuration, e.g., access to the same number of samples. We can witness that local SGD could achieve similar performance as mini-batch SGD, while enjoying the benefits of less communication traffic. The performance of local SGD could be further improved while keeping the property of communication efficiency, following the configurations [3] mentioned in Section 4.2 and Section E.

	CIFAR-10		CIFAR-100	
	Test Top-1 Accuracy	Running Time (hour)	Test Top-1 Accuracy	Running Time (hour)
ResNet-20 (K=2, H=1)	92.40 ± 0.03	2.42	68.84 ± 0.06	2.47
ResNet-20 (K=2, H=8)	92.23 ± 0.04	1.55	68.03 ± 0.04	1.55
DenseNet-40-12 (K=2, H=1)	94.33 ± 0.14	5.25	73.84 ± 0.14	5.27
DenseNet-40-12 (K=2, H=8)	94.00 ± 0.16	3.77	73.53 ± 0.12	3.78
WideResNet-28-10 (K=2, H=1)	95.73 ± 0.00	18.15	78.77 ± 0.16	19.08
WideResNet-28-10 (K=2, H=8)	95.57 ± 0.10	12.30	78.19 ± 0.02	12.78

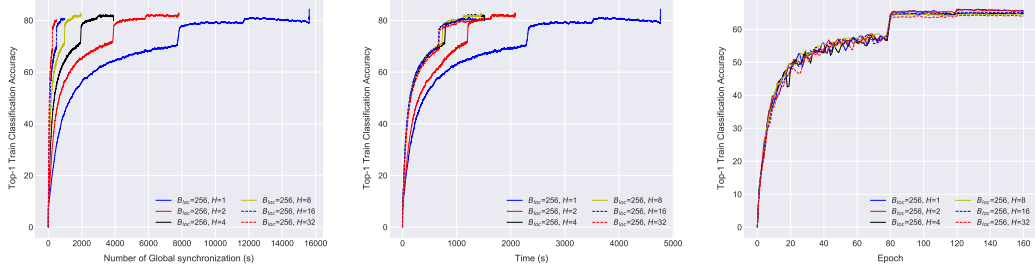
D.2.2 Small Scale Local SGD Experiments

Figure 7 trains CIFAR-100 with ResNet-20 via local SGD on 2×1 -GPU.

D.2.3 Additional Experiments - When does averaging help?

The paper [7] investigates the effect of averaging for CNN on MNIST. They state that “One-shot averaging degrades performance compared to single worker performance while periodic averaging improves the results”. Our work on top of it and investigates the impact of local step, or more precisely, the averaging frequency, on the final test performance through CIFAR-10 on ResNet-20 (i.e., Table 6 and Table 7).

It is quite interesting for the top-1 test accuracy of 2-GPU case that it first slightly decreases by increasing local step H and then shows an upward trend when we have less frequent model averaging. The result of Table 7 shows a similar observation. Moreover, we could further conclude that for



(a) Training accuracy vs. global sync. (b) Training accuracy vs. training time. (c) Test accuracy vs. training time.

Figure 7: Train **CIFAR-100** via **Local SGD** on 2×1 -GPU. The local batch size B_{loc} is fixed to 256 for CIFAR-100, and the local step is varied from 1 to 32.

cluster with a large number of computing units, local SGD with a large number of local steps cannot significantly reduce the communication cost, which might result from the increased synchronization time for processes with too independent parallel local steps. For this limitation of local SGD, hierarchical local SGD would be an excellent alternative solution to ensure the trade-off between model performance and training time.

Table 6: Training **CIFAR-10** with **ResNet-20** via **local SGD** on 2×1 -GPU. The local batch size B_{loc} is fixed to 128 and we scale the local step H from 1 to 1024. The reported results are the average of three runs and all the experiments are under the same configuration.

H	1	2	4	8	16	32	64	128	256	512	1024
Test Top-1 Accuracy (%)	92.47 \pm 0.16	92.31 \pm 0.06	92.27 \pm 0.04	92.05 \pm 0.17	91.63 \pm 0.13	91.57 \pm 0.19	91.61 \pm 0.18	91.66 \pm 0.18	91.82 \pm 0.10	91.97 \pm 0.07	91.99 \pm 0.07

Table 7: Training **CIFAR-10** with **ResNet-20** via **local SGD** on a 5×2 -GPU Kubernetes cluster. The local batch size B_{loc} is fixed to 128 with $H^b = 1$, and we scale the local step H from 1 to 1024. The reported results are the average of three runs and all the experiments are under the same configuration.

H	1	2	4	8	16	32	64	128	256	512	1024
Test Top-1 Accuracy (%)	92.55 \pm 0.11	91.09 \pm 0.26	90.51 \pm 0.18	90.01 \pm 0.29	88.32 \pm 0.30	88.48 \pm 0.08	87.82 \pm 0.21	87.45 \pm 0.17	87.34 \pm 0.17	87.39 \pm 0.27	87.66 \pm 0.11
Training Time (minutes)	20.07	13.95	10.48	9.20	8.57	8.32	9.22	9.23	9.5	10.30	10.65

E Practical Improvements to Local SGD Training

E.1 When Local SGD meets Momentum Schemes

Momentum mini-batch SGD is widely used in place of vanilla SGD. The distributed mini-batch SGD with vanilla momentum on K training nodes follows

$$u_{(t)} = mu_{(t-1)} + \frac{1}{K} \sum_{k=1}^K \nabla_{(t)}^k, \quad w_{(t+1)} = w_{(t)} - \gamma u_{(t)}$$

where $\nabla_{(t)}^k = \frac{1}{|\mathcal{I}_{(t)}^k|} \sum_{i \in \mathcal{I}_{(t)}^k} \nabla f_i(w_{(t)})$.

After H updates of mini-batch SGD, we have the following updated $w_{(t+H)}$:

$$w_{(t+H)} = w_{(t)} - \gamma \left(\sum_{\tau=1}^H m^\tau u_{(\tau-1)} + \sum_{\tau=0}^{H-1} \frac{m^\tau}{K} \sum_{k=1}^K \nabla_{(t)}^k + \dots + \sum_{\tau=0}^0 \frac{m^\tau}{K} \sum_{k=1}^K \nabla_{(t+H-1)}^k \right)$$

Coming back to the setting of local SGD, it is straightforward that we can apply momentum acceleration on each local model, or on global level [21]. In the left of this section, we analyze the case of applying local momentum and global momentum. For ease of understanding, we assume the learning rate γ is the same throughout the H update steps.

E.1.1 Local SGD with Local Momentum

When applying local momentum on the local SGD, i.e., use independent identical momentum acceleration for each local model and only globally aggregate the gradients at the time $(t) + H$, we have the following local update scheme

$$u_{(t)}^k = mu_{(t-1)}^k + \nabla_{(t)}^k, \quad w_{(t)+1}^k = w_{(t)}^k - \gamma u_{(t)}^k,$$

where $\nabla_{(t)}^k = \frac{1}{|\mathcal{I}_{(t)}^k|} \sum_{i \in \mathcal{I}_{(t)}^k} \nabla f_i(w_{(t)})$. Consequently, after H local update steps,

$$w_{(t)+H}^k = w_{(t)}^k - \gamma \left(\sum_{\tau=1}^H m^\tau u_{(\tau-1)}^k + \sum_{\tau=0}^{H-1} m^\tau \nabla_{(t)}^k + \dots + \sum_{\tau=0}^0 m^\tau \nabla_{(t+H-1)}^k \right).$$

Substuite above equation to (4), we have

$$\begin{aligned} w_{(t+1)} &= w_{(t)} - \frac{1}{K} \sum_{k=1}^K \gamma \left(\sum_{\tau=1}^H m^\tau u_{(\tau-1)}^k + \sum_{\tau=0}^{H-1} m^\tau \nabla_{(t)}^k + \dots + \sum_{\tau=0}^0 m^\tau \nabla_{(t+H-1)}^k \right) \\ &= w_{(t)} - \gamma \left(\sum_{\tau=1}^H \frac{m^\tau}{K} \sum_{k=1}^K u_{(\tau-1)}^k + \sum_{\tau=0}^{H-1} m^\tau \left(\frac{1}{K} \sum_{k=1}^K \nabla_{(t)}^k \right) + \dots + \sum_{\tau=0}^0 \frac{m^\tau}{K} \sum_{k=1}^K \nabla_{(t+H-1)}^k \right) \end{aligned}$$

Compare the mini-batch SGD with local momentum local SGD after H update steps (H global update steps V.S. H local update steps and 1 global update step), we can witness that the main difference of these two update schemes is the difference between $\sum_{\tau=1}^H m^\tau u_{(\tau-1)}$ and $\sum_{\tau=1}^H \frac{m^\tau}{K} \sum_{k=1}^K u_{(\tau-1)}^k$, where mini-batch SGD hold a global $u_{(t-1)}$ while each local model of the local SGD has their own $u_{(t-1)}^k$. We will soon see the difference between the global momentum of mini-batch SGD and the local momentum of local SGD.

E.1.2 Local SGD with Global Momentum

For global momentum local SGD, i.e., a more general variant of block momentum [21], we would like to only apply the momentum factor to the accumulated/synchronized gradients:

$$\begin{aligned} u_{(t)} &= mu_{(t-1)} + \frac{1}{\gamma} \sum_{k=1}^K \frac{1}{K} (w_{(t)}^k - w_{(t)+H}^k) = mu_{(t-1)} + \frac{1}{\gamma} \sum_{k=1}^K \frac{1}{K} \sum_{l=0}^{H-1} \gamma \nabla_{(t)+l}^k, \\ w_{(t+1)} &= w_{(t)} - \gamma u_{(t)} = w_{(t)} - \gamma \left(mu_{(t-1)} + \sum_{l=0}^{H-1} \sum_{k=1}^K \frac{1}{K} \nabla_{(t)+l}^k \right) \end{aligned}$$

where $w_{(t)+H}^k = w_{(t)}^k - \eta \sum_{l=0}^{H-1} \nabla_{(t)+l}^k = w_{(t)} - \eta \sum_{l=0}^{H-1} \nabla_{(t)+l}^k$. Note that for local SGD, we consider summing the gradients from each local update, i.e., the model difference before and after one global synchronization, and then apply the global momentum to the gradients over workers over previous local update steps.

Obviously, there exists a significant difference between mini-batch momentum SGD and global momentum local SGD, at least the term $\sum_{\tau=0}^H m^\tau$ is canceled.

E.1.3 Local SGD with Hybrid Momentum

The following equation tries to combine local momentum with global momentum, which shows how the naive implementation of local momentum and global momentum will be.

First of all, based on the local momentum scheme, after H local update steps,

$$w_{(t)+H}^k = w_{(t)}^k - \gamma \left(\sum_{\tau=1}^H m^\tau u_{(t-1)}^k + \sum_{\tau=0}^{H-1} m^\tau \nabla_{(t)}^k + \dots + \sum_{\tau=0}^0 m^\tau \nabla_{(t)+H-1}^k \right)$$

Together the result from local momentum with the global momentum, we have

$$\begin{aligned} u_{(t)} &= mu_{(t-1)} + \frac{1}{\gamma} \sum_{k=1}^K \frac{1}{K} (w_{(t)}^k - w_{(t)+H}^k) \\ w_{(t+1)} &= w_{(t)} - \gamma u_{(t)} = w_{(t)} - \gamma \left[mu_{(t-1)} + \frac{1}{\gamma} \sum_{k=1}^K \frac{1}{K} (w_{(t)}^k - w_{(t)+H}^k) \right] \\ &= w_{(t)} - \gamma \left[mu_{(t-1)} + \sum_{\tau=1}^H \frac{m^\tau}{K} \sum_{k=1}^K u_{(t-1)}^k + \sum_{\tau=0}^{H-1} \frac{m^\tau}{K} \sum_{k=1}^K \nabla_{(t)}^k + \dots + \sum_{\tau=0}^0 \frac{m^\tau}{K} \sum_{k=1}^K \nabla_{(t)+H-1}^k \right] \end{aligned}$$

where $u_{(t-1)}$ is the global momentum memory and $u_{(t-1)}$ is the local momentum memory for each node k .

E.1.4 Local SGD with Momentum in Practice

In practice, it is suggested to combine the local momentum with global momentum to further improve the model performance. We slightly investigate the impact of momentum scheme on CIFAR-10 trained with ResNet-20 on a 5×2 -GPU cluster, e.g., in Table 8 and Table 9. For more works that are relevant to the momentum scheme of local SGD, please refer to [21, 20].

Table 8 indicates that some factors of global momentum could further slightly improve the final test accuracy. More estimation w.r.t. different local update steps of the local SGD training can refer to Table 9.

Table 8: Evaluate local momentum and global momentum for **ResNet-20** on **CIFAR-10** data via local SGD training ($H = 1$ case) on 5×2 -GPU Kubernetes cluster. The local mini-batch size is 128 and base batch size is 64 (used for learning rate linear scale). Each local model will access to a disjoint data partition, using the standard learning rate scheme as [39].

local momentum	global momentum	test top-1 (10 GPUs)
0.0	0.0	90.57
0.9	0.0	92.41
0.9	0.1	92.22
0.9	0.2	92.09
0.9	0.3	92.54
0.9	0.4	92.45
0.9	0.5	92.19
0.9	0.6	91.32
0.9	0.7	18.76
0.9	0.8	14.35
0.9	0.9	12.21
0.9	0.95	10.11

Table 9: Brief performance evaluation of local momentum and global momentum on local SGD training, for **ResNet-20** with **CIFAR-10** data on 5×2 -GPU Kubernetes cluster. The local mini-batch size is 128 and base batch size is 64 (used for learning rate linear scale). Each local model will access to a disjoint data partition, using the standard learning rate scheme as [39].

	$H = 8$
local momentum=0.9, global momentum=0.0	89.97
local momentum=0.9, global momentum=0.1	90.22
local momentum=0.9, global momentum=0.2	90.25
local momentum=0.9, global momentum=0.3	90.23
local momentum=0.9, global momentum=0.4	90.24
local momentum=0.9, global momentum=0.5	90.15